

# Ligand based virtual screening and biological evaluation of inhibitors of chorismate mutase (Rv1885c) from *Mycobacterium tuberculosis* H37Rv

Himanshu Agrawal,<sup>†</sup> Ashutosh Kumar,<sup>†</sup> Naresh Chandra Bal,  
Mohammad Imran Siddiqi and Ashish Arora<sup>\*</sup>

*Molecular and Structural Biology, Central Drug Research Institute, Lucknow 226 001, India*

Received 7 November 2006; revised 28 February 2007; accepted 16 March 2007  
Available online 21 March 2007

**Abstract**—We have identified new lead candidates that possess inhibitory activity against *Mycobacterium tuberculosis* H37Rv chorismate mutase by a ligand-based virtual screening optimized for lead evaluation in combination with in vitro enzymatic assay. The initial virtual screening using a ligand-based pharmacophore model identified 95 compounds from an in-house small molecule database of 15,452 compounds. The obtained hits were further evaluated by molecular docking and 15 compounds were short listed based on docking scores and the other scoring functions and subjected to biological assay. Chorismate mutase activity assays identified four compounds as inhibitors of *M. tuberculosis* chorismate mutase (MtCM) with low  $K_i$  values. The structural models for these ligands in the chorismate mutase binding site will facilitate medicinal chemistry efforts for lead optimization against this protein.

© 2007 Elsevier Ltd. All rights reserved.

Tuberculosis (TB) kills more than two million people a year worldwide (<http://www.avert.org/tuberc.htm>).<sup>1</sup> The emergence of multiple-drug-resistant TB and its synergism with HIV is a burgeoning threat which compels characterization of new enzyme targets and the development of new drugs (<http://www.avert.org/tuberc.htm>).

Chorismate mutase (EC 5.4.99.5) catalyzes the Claisen rearrangement of chorismate to prephenate (Fig. 1) in the shikimate pathway which leads to the synthesis of the aromatic amino acids phenylalanine and tyrosine. This is the single known example of an enzyme catalyzing a pericyclic reaction.

Shikimate pathway for the biosynthesis of aromatic compounds is evidently present in bacteria, fungi, and plants but absent in animals. Therefore, chorismate mutase is a novel target for generation of antibiotics, fungicides, and herbicides.<sup>2</sup>

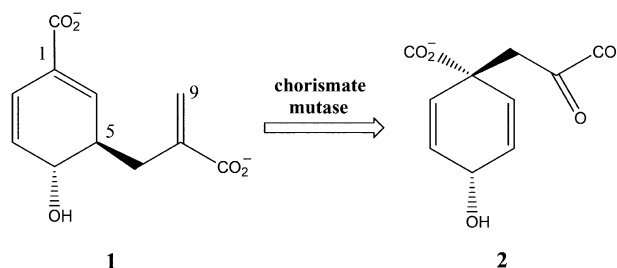


**Figure 1.** Claisen rearrangement of chorismate to prephenate.

*Mycobacterium tuberculosis* H37Rv genome contains two genes (Rv1885c and Rv0948c) responsible for chorismate mutase activity.<sup>3</sup> The protein encoded by Rv1885c has been characterized as a mono-functional chorismate mutase (MtCM) having an N-terminal signal sequence (1–33 residues). While the shikimate pathway is commonly present in the cytoplasm of bacteria and higher plants, MtCM is secreted out of the cell to provide support to *M. tuberculosis* in aromatic amino acid deficient medium.<sup>4</sup> It has also been proposed recently that MtCM might interact with the host macrophages and might be important in virulence.<sup>5</sup> On the other hand, the protein encoded by Rv0948c is a bifunctional

**Keywords:** *Mycobacterium tuberculosis*; Chorismate mutase; Virtual screening; Molecular docking; Biological evaluation.

<sup>\*</sup> Corresponding author. E-mail: [ashishcdri@yahoo.com](mailto:ashishcdri@yahoo.com)

<sup>†</sup> Both authors have contributed equally.

chorismate mutase-prephenate dehydratase, that lacks a signal sequence and is, therefore, restricted to the cytoplasm. Moreover, it has been shown that Rv1885c is the major contributor toward the CM activity of the cell, while Rv0948c is only a minor contributor.<sup>3</sup> For our study we have used the recently solved crystal structure of MtCM (Rv1885c) (PDB ID—2F6L).<sup>6</sup>

We have employed an integrated database screening strategy involving two popular 3D-database screening approaches: pharmacophore hypothesis based 3-D database search and protein structure-based docking approach. Since there are no known inhibitors of MtCM, we developed the ligand-based pharmacophore model based on the substrate chorismic acid and three aza inhibitors (Fig. 2) of chorismate mutase from *Saccharomyces cerevisiae*,<sup>7</sup> as the active sites of these two proteins are quite similar.<sup>6</sup> The pharmacophore model was derived by means of a genetic algorithm similarity program GASP.<sup>8</sup> The program employs a genetic algorithm for determining the correspondence between functional groups in the superimposed ligands and the alignment of these groups in a common geometry for receptor binding. Pharmacophore model generated by GASP consists of positions and tolerance for four acceptor sites, AA1–AA4 (Fig. 3). This model was used to perform a pharmacophore search of 3-D compound database to identify ‘hits’ that satisfy the chemical and the geometrical requirements using UNITY module of Sybyl7.1. The CDRI small molecule repository<sup>9</sup> and database consist of 15,659 molecules out of which 15,452 conform to the modified Lipinski’s rule of 5.<sup>10</sup> Only the filtered subset of 15,452 molecules was used for the screening. Virtual screening with UNITY using ligand-based pharmacophore model yielded 95 hits that met the specified requirements. Finally, protein structure-based molecular docking was used to dock each ‘hit’ to the active site of chorismate mutase and

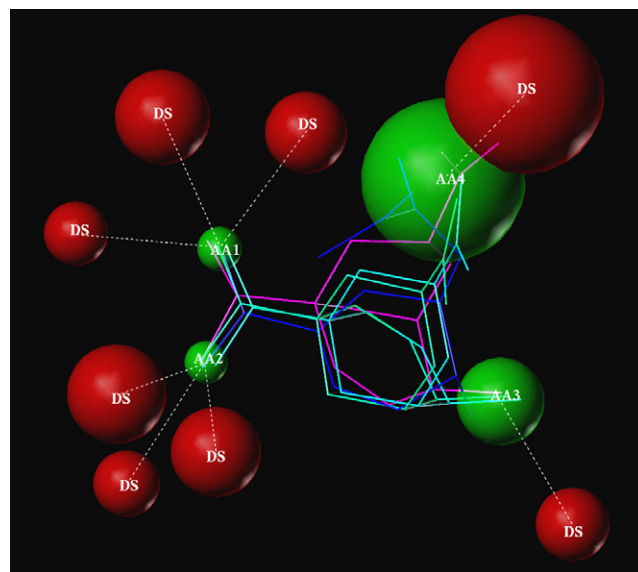


**Figure 3.** The GASP model for Chorismate mutase inhibitors containing four acceptor atoms shown in green spheres. Red spheres represent the donor sites. The sphere sizes indicate query tolerances.

to rank the binding affinities. FlexX<sup>11</sup> based molecular docking study was carried out to perform scoring and ranking of the hits obtained from database searching. FlexX method of molecular docking involves incremental construction of ligands from smaller fragments in the cavity of a receptor. All the hits obtained in database searching were docked into the inhibitor binding site in the X-ray crystal structure of MtCM (PDB Accession No. 2F6L). The active site in the MtCM was searched using SiteID module of Sybyl7.1<sup>12</sup> and the probable active site determination was accomplished based on previously reported structural information.<sup>6</sup> For a comparative analysis of the hits obtained in database

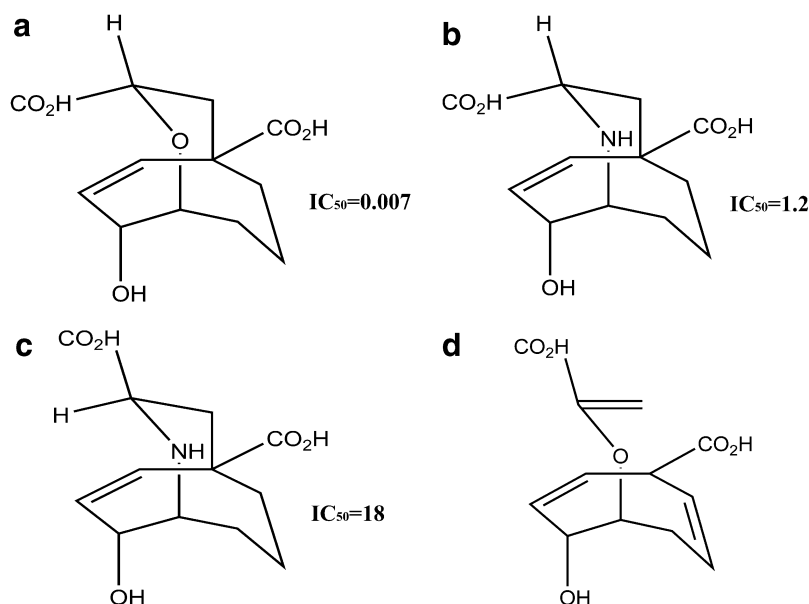


**Figure 2.** *Saccharomyces cerevisiae* chorismate mutase inhibitors (a–c) and the substrate chorismic acid (d) used for pharmacophore model generation.

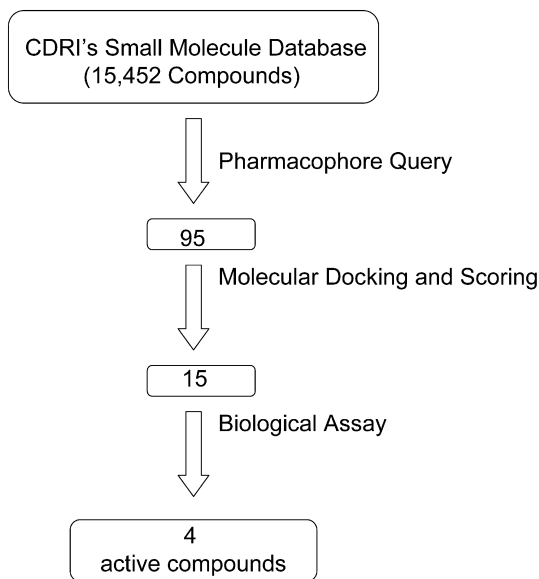


**Figure 4.** Flow chart indicating the results obtained from the virtual screening of CDRI small molecule database. The numbers given in the figure represent the number of molecules selected after each stage.

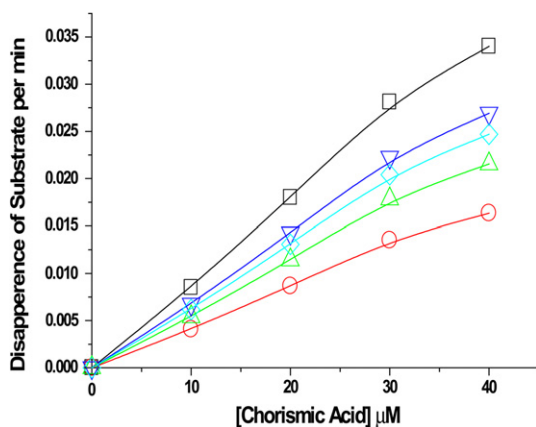


**Figure 5.** Initial rates of the conversion of chorismic acid to prephenic acid. Reaction was started by the addition of 10 pmol MtCM to pre-warmed 100  $\mu\text{M}$  chorismic acid, in the presence or absence of different inhibitors. The concentration of inhibitor used was 100 nM. Without inhibitor ( $\square$ ), With compound I ( $\circ$ ), With compound II ( $\triangle$ ), with compound III ( $\diamond$ ), with compound IV (+).

searching, FlexX score,<sup>13</sup> G\_score,<sup>14</sup> PMF\_score,<sup>15</sup> D\_score<sup>16</sup>, and Chem\_score<sup>17</sup> were estimated using the C-score module of the Sybyl7.1.<sup>12</sup> CScore program accesses the above scoring functions and combines individual scores into a consensus score. The combined scoring functions perform in a superior fashion to the single scoring function and by their nature the combination of functions will ameliorate the effect of any particularly unsuitable single function.

At the final stage, 15 molecules having FlexX energy scores from  $-25$  to  $-3$  kJ/mol and with C-score values of 5 were selected. The selected molecules displayed a good binding mode characterized by interactions of the hydrogen bond acceptors in the ligands with the

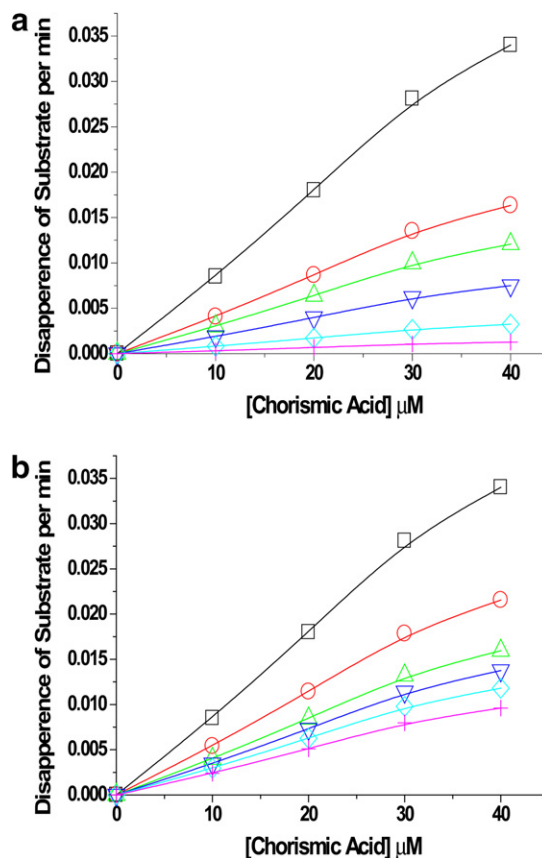


**Figure 6.** Initial rates of conversion of chorismic acid to prephenic acid. Reaction was started by the addition of 10 pmol MtCM to pre-warmed 100  $\mu\text{M}$  chorismic acid, in the presence or absence of different concentrations (0–100  $\mu\text{M}$ ) of (a) inhibitor I, and (b) inhibitor II. Without inhibitor ( $\square$ ), with 100 nM inhibitor ( $\circ$ ), with 1  $\mu\text{M}$  inhibitor ( $\triangle$ ), with 10  $\mu\text{M}$  inhibitor ( $\nabla$ ), with 50  $\mu\text{M}$  inhibitor ( $\diamond$ ), and with 100  $\mu\text{M}$  inhibitor (+).

hydrogen bond donor sites of the protein, which was analyzed visually. The values for various scores for these 15 compounds are given in Table 2 (supporting information). These compounds were retrieved from CDRI small molecule repository and subjected to biological evaluation (Fig. 4).

The 15 selected compounds after virtual screening were further screened biologically.<sup>18</sup> Our results show that four inhibitors, that is, compound number I, II, III, and IV, inhibit enzymatic activity by competitive inhibition. Figure 5 shows differences in initial rates of the enzyme activity in the absence and presence of the inhibitors. These inhibitors do not alter  $V_{\text{max}}$  at the higher concentration of substrate (chorismic acid) in the range of 1–5 mM. However, they do increase the  $K_m$ , which is denoted as apparent  $K_m$ . Dissociation constant for inhibitor binding ( $K_i$ ) values were determined by plotting the apparent  $K_m$  values against the respective inhibitor concentration using Eq. 1.

$$K_m(\text{apparent}) = K_m(1 + [I]/K_i). \quad (1)$$

Data were plotted using Michaelis–Menten kinetics in Graph Pad Prism. Similarly, mode of inhibition was

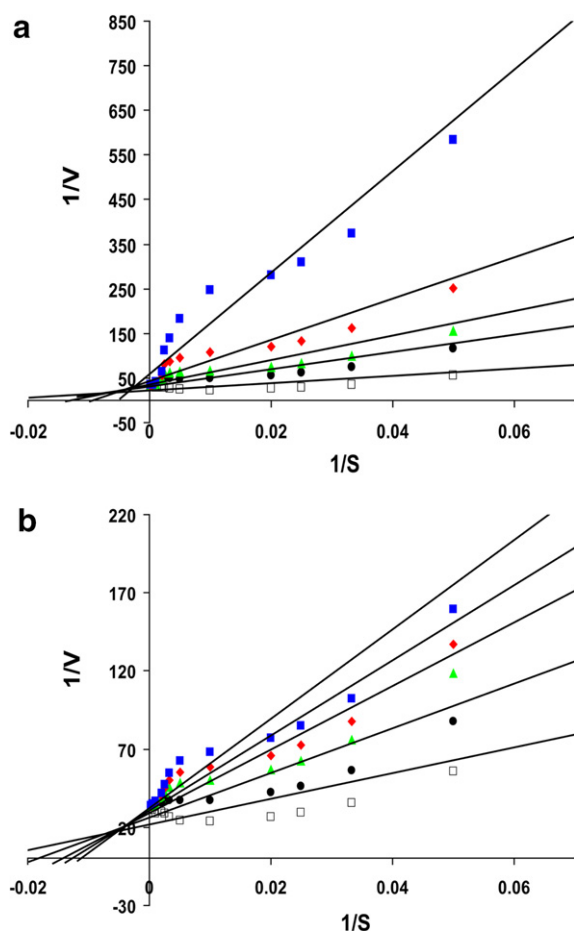


**Figure 7.** Competitive inhibition of MtCM with respect to chorismic acid by the selected compounds **I** and **II**. Data were fitted using standard linear regression. The double-reciprocal plots clearly indicate competitive binding between chorismic acid and compounds (a) **I** and (b) **II**. Activity of MtCM was measured in the presence of increasing concentrations of inhibitor compound in the range of 0–100  $\mu\text{M}$ .

determined through standard analysis of Lineweaver–Burk kinetics.

In Figure 6, the behavior of two of the most potent inhibitors against MtCM is shown. Double reciprocal plots and linear regression fit to the data, in the presence of different concentrations of compounds **I** and **II**, for the determination of apparent  $K_m$  are shown in Figure 7a and b, respectively. From linear regression fitting to Eq. 1,  $K_i$  values for compounds **I** and **II** were found to be 5.7 and 17  $\mu\text{M}$ , respectively. The compounds **III** and **IV** also showed  $K_i$  values in  $\mu\text{M}$  range and are shown in Table 1. However, rest of the compounds listed in Table 2 (supporting information) were found to be inactive.

To understand the mechanism underlying the inhibition of MtCM by the selected compounds, we analyzed the docking modes of active inhibitors **I** and **II**, in the active site of MtCM. The inhibitors appear to fit well in the active site pocket showing several hydrogen-bonding and van der Waals interactions with the binding site residues. The binding conformation of compounds **I** and **II** is shown in Figure 8.

The oxygen atoms of sulfate group of compound **I**, corresponding to acceptor sites AA1 and AA2 of pharmacophore model (Fig. 3), act as hydrogen bond acceptor for the side-chain N–H of Lys60 (distance 2.4 Å) and side-chain nitrogen of Gln76 (distance 1.956 Å). Side-chain carbonyl group of Gln76 also makes hydrogen bond with nitrogen atom of compound **I** (distance 2.292 Å). Similarly, oxygen atom of nitro group of compound **I**, which maps to AA3 of the pharmacophore model, interacts with guanidinium nitrogen of Arg49. The results indicate that the nitro group substituted at *meta* position of phenyl ring plays an important role

**Table 1.** List of active inhibitors with molecular weight and calculated  $K_i$  values

Compound	Chemical structure	Molecular weight	$K_i$ ( $\mu\text{M}$ )
<b>I</b>		425.09	$5.7 \pm 1.2$
<b>II</b>		363.75	$17.71 \pm 3.35$
<b>III</b>		422.19	$21.1 \pm 3.6$
<b>IV</b>		210.19	$28.8 \pm 4.1$



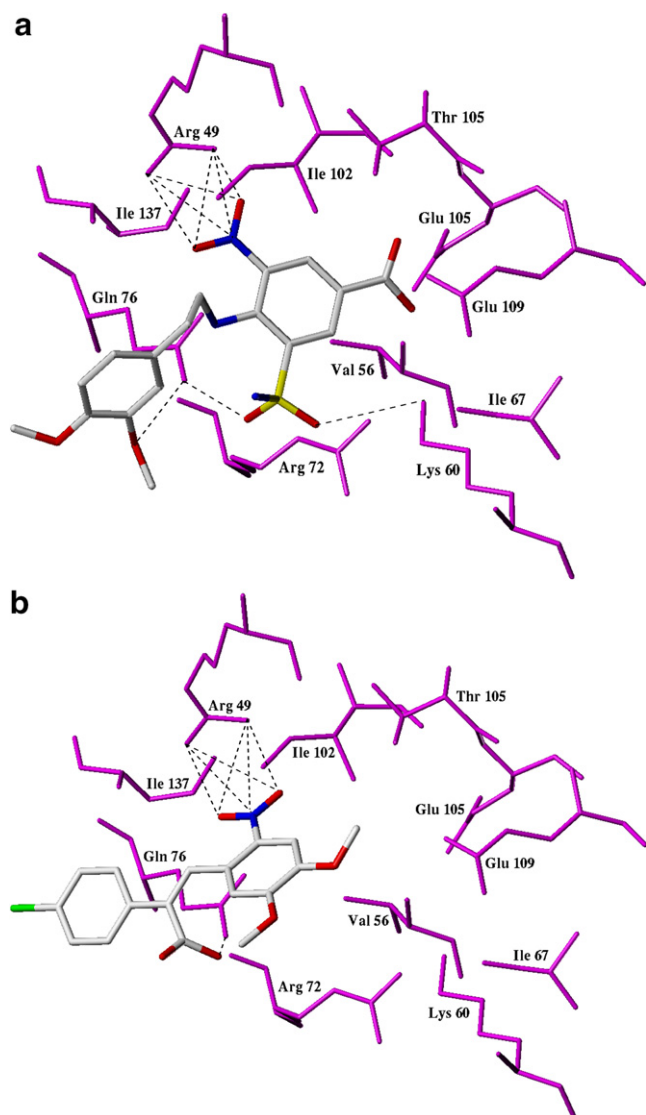


**Figure 8.** Docked conformation of (a) **I** and (b) **II** in the catalytic site of MtCM X-ray crystal structure.

in binding to chorismate mutase. A similar mode of binding is also observed for the binding of compound **II**, where the nitro group interacts extensively with side-chain nitrogen of Arg49. Furthermore, most of the hydrophobic interactions between MtCM and inhibitors were conserved within the docking mode of compounds **I** and **II**. Thus, Val56, Arg72, Ile102, and Ile137 were found to form hydrophobic contacts with molecules **I** and **II**. However, the oxygen atom of these two inhibitors which corresponds to the AA4 feature of the pharmacophore model was not found to be involved in any hydrogen bonding interaction.

In summary, we have successfully performed virtual screening of in-house small molecule database of 15,452 available chemicals to search for MtCM inhibitors. We utilized ligand-based pharmacophore modeling and screening of small molecule database. We have successfully identified four novel compounds for the inhibition of MtCM. Particularly, compound **I** showed the

most potent inhibition with  $K_i$  value of 5.7  $\mu$ M against MtCM. The docking studies performed in the binding pocket of X-ray crystal structure of MtCM reveal the interactions that are important for binding to the enzyme. The experimental validation of our pharmacophore model will advance further efforts for lead optimization by chemical derivatization of active compounds identified in this study.

### Acknowledgments

Biological work involved in this project was supported by Council of Scientific and Industrial Research (CSIR) funded network project SMM003. Computational work involved in this project was supported by Council of Scientific and Industrial Research (CSIR) funded network project CMM0017-Drug target development using in-silico biology. HA, AK, and NCB acknowledge CSIR for fellowship. C.D.R.I. communication number of this manuscript is 7097.

### Supplementary data

Supplementary data associated with this article can be found, in the online version, at [doi:10.1016/j.bmcl.2007.03.053](https://doi.org/10.1016/j.bmcl.2007.03.053).

### References and notes

- World Health Organization. WHO report **2006**, Geneva, (WHO/HTM/TB/2006.362).
- Haslam, E. *Shikimic Acid: Metabolism and Metabolites*; Wiley: New York, 1993.
- Prakash, P.; Aruna, B.; Sardesai, A. A.; Hasnain, S. E. *J. Biol. Chem.* **2005**, *280*, 19641.
- Sasso, S.; Ramakrishnan, C.; Gamper, M.; Hilvert, D.; Kast, P. *FEBS J.* **2005**, *272*, 375.
- Qamra, R.; Prakash, P.; Aruna, B.; Hasnain, S. E.; Mande, S. C. *Biochemistry* **2006**, *45*, 6997.
- Okvist, M.; Dey, R.; Sasso, S.; Grah, E.; Kast, P.; Krengel, U. *J. Mol. Biol.* **2006**, *357*, 1483.
- Hediger, M. E. *Bioorg. Med. Chem.* **2004**, *12*, 4995.
- Jones, G.; Willett, P.; Glen, R. C. *J. Comput. Aided Mol. Des.* **1995**, *9*, 532.
- The CDRI repository has 15,659 pure compounds collected over four decades from in-house chemical synthesis. These compounds were selected from ~150,000 synthesized compounds on the basis of their activity in enzyme-based and cell-based assays under various drug discovery programs.
- Lipinski, C. A.; Lombardo, F.; Dominy, B. W.; Feeney, P. *J. Adv. Drug Delivery Rev.* **2001**, *46*, 3.
- Flex X, version 1.13.5; Saint Augustin, Germany, BioSolveIT GmbH.
- TRIPOS Inc. 1699, South Hanley Road, St. Louis, MO 63144, USA.
- Rarey, M.; Kramer, B.; Lengauer, T.; Klebe, G. *J. Mol. Biol.* **1996**, *261*, 470.
- Jones, G.; Willett, P.; Glen, R. C.; Leach, A. R.; Taylor, R. *J. Mol. Biol.* **1997**, *267*, 727.
- Muegge, I.; Martin, Y. C. *J. Med. Chem.* **1999**, *42*, 791.
- Ewing, T. J. A.; Kuntz, I. D. *J. Comput. Chem.* **1997**, *18*, 1175.

17. Eldridge, M. D.; Murray, C. W.; Auton, T. R.; Paolini, G. V.; Mee, R. P. *J. Comput. Aided Mol. Des.* **1997**, 11425.
18. Biological assay—MtCM gene was PCR amplified and cloned into expression vector pET22b (Novagen) and labeled as pET22b/mtCM. MtCM was purified from over-expressed culture of BL21 ( $\lambda$ DE3) harboring pET22b/mtCM by Ni-NTA affinity chromatography. Activity of chorismate mutase enzyme is based on the direct observation of conversion of chorismate to prephenate spectrophotometrically at OD274. The reaction volume of 100  $\mu$ l contained 50 mM phosphate buffer, pH 6.5, and chorismic acid 10  $\mu$ M to 5 mM. The reaction was started by adding 10 pmol of purified protein to the pre-warmed chorismic acid solution. Inhibitory screening of all selected ligands against chorismate mutase activity was measured at 100 nM to 100  $\mu$ M concentrations of the effectors.